Casimir stress in materials: Hard divergency at soft walls

Itay Griniasty and Ulf Leonhardt
Department of Physics of Complex Systems, Weizmann Institute of Science, Rehovot 761001, Israel
(Received 10 April 2017; revised manuscript received 25 October 2017; published 10 November 2017)

The Casimir force between macroscopic bodies is well understood, but not the Casimir stress inside bodies. Suppose empty space or a uniform medium meets a soft wall where the refractive index is continuous but its derivative jumps. For this situation we predict a characteristic power law for the stress inside the soft wall and close to its edges. Our result shows that such edges are not tolerated in the aggregation of liquids at surfaces, regardless whether the liquid is attracted or repelled.

DOI: 10.1103/PhysRevB.96.205418

I. INTRODUCTION

In 1948 Casimir [1] found an enigmatic formula for the part of the zero-point energy density of the electromagnetic field between two perfect mirrors that can do physical work:

$$U = \frac{\pi^2}{240}\frac{\hbar c}{a^4}, \tag{1}$$

where a is the distance between the mirrors, $\hbar$ Planck's constant divided by 2π, and c the speed of light in vacuum. These days, nearly 70 years later, the field of Casimir forces is an established research area where modern theory [2,3] can predict the results of high-precision experiments with good accuracy. The Casimir force *between* macroscopic bodies is well understood, but surprisingly [4], not the force *inside* bodies. Only very recently, after several attempts [5,6] of establishing a theory of the Casimir stress inside materials, one was found [7] that appears to be satisfactory. Here we report on the first prediction of that theory: The Casimir stress σ near the edge of a soft wall [8] (Fig. 1) behaves like

$$\sigma_{zz} = \frac{23}{240\,(2\pi)^2}\frac{\hbar c}{a^2 b^2}, \tag{2}$$

where σ_{zz} is the physically relevant stress component and a denotes the distance from the edge to empty space. Here the refractive index n changes continuously along the z coordinate while its first derivative jumps by $1/b$ [Fig. 1(a)].

Equation (2) shows that at discontinuities of the derivative of n, the Casimir stress diverges with a characteristic power law. The power law follows already from dimensional analysis: To get a stress with the dimensions of an energy density one has to divide $\hbar c$ by the fourth power of lengths. There are two lengths, a and b, that the stress near an edge must depend on. As the stress must vanish far from the edge, or when there is no jump, there are three physically reasonable scaling behaviors $\sigma_{zz} \sim 1/ab^3$,$1/a^2b^2$, or $1/a^3b$. Our result, Eq. (2), is one of them. Note that there is a body of work on the Casimir effect of soft walls [8]; none, however, got these scaling behaviors.

At discontinuities of the derivative of n, the Casimir stress diverges with a power law. In contrast, at discontinuities of n itself, σ_{zz} does not diverge, but merely jumps [9], and gives Eq. (1) for two plates with $n \to \infty$. Note that the divergency of the stress at the edge of the soft wall is a physical effect, not an artefact of the infinite bare zero-point energy that is removed in the renormalization of the Casimir force [7]. The infinite physical stress at the edge implies that a discontinuity of the derivative of n is not tolerated in liquids: if, for example, a liquid aggregates as a soft wall on a boundary,

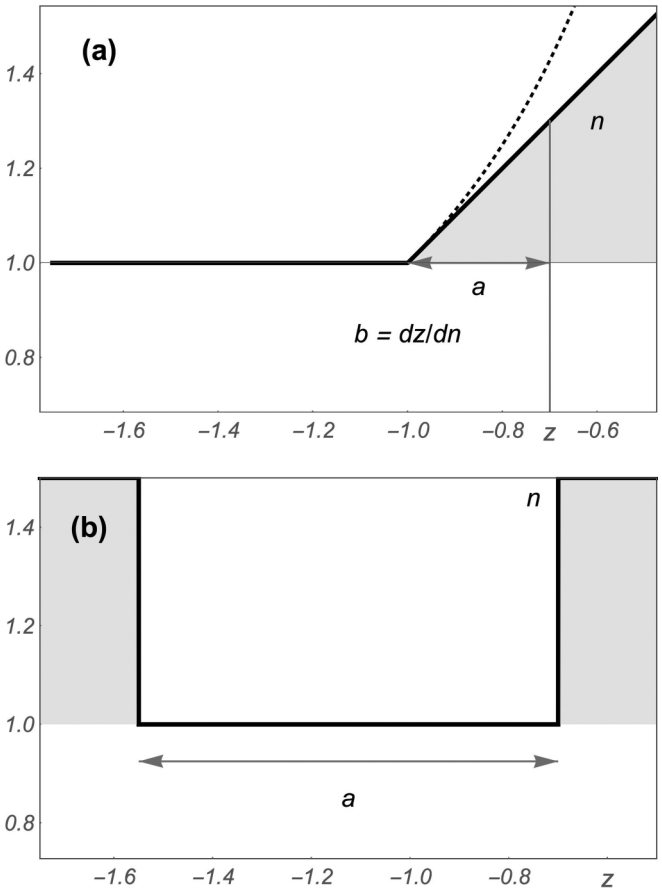

FIG. 1. Soft versus hard wall. (a) Soft wall. Refractive-index profile $n(z)$ of a planar material where the first derivative of n jumps by $1/b$ at the edge to free space with $n = 1$. Equation (2) describes the Casimir stress near the edge with a being the distance from the edge. The dotted line indicates the Beltrami profile of Eq. (7), fitting the actual profile at the edge, employed to calculate the stress analytically. (b) The hard walls of a cavity of length a generate the Casimir energy, Eq. (1), in the limit of perfect mirrors, $n \to \infty$.

such discontinuities are immediately removed by the force density $\nabla \cdot \sigma$ putting the liquid into motion. Discontinuities of n, on the other hand, are locally stable, leading only to forces between bodies and not to tension inside. Our result thus shows a striking feature in the aggregation process: regardless whether n rises or falls, i.e., Regardless whether the Casimir force is attractive or repulsive [10], a liquid cannot tolerate the edge of a soft wall; preferably it will form a discontinuity of the refractive index: either it will be aggregated or repelled. This application of the theory of Casimir forces inside materials [7] resembles the early tests of the Lifshitz theory [11] of forces between materials in the wetting of surfaces [12]. There the Casimir stress at the interface between a liquid and a solid wall gives the wetting angles of droplets on the surface; here the Casimir stress inside the liquid describes the consolidation of surfaces.

We proceed as follows. In Sec. II we briefly review the theory [7] of the Casimir stress in planar inhomogeneous media, including the renormalization, setting the scene for Casimir forces inside soft walls. In Sec. III we take ideas from geometry that simplify the renormalization. With these geometric insights and with the help of asymptotic considerations, we derive our analytic result Eq. (2) in Sec. IV. There we make an additional assumption: We presume that the Casimir stress density near the edge of the soft wall is dominated by discontinuities of the derivative of the refractive index. Equation (2) is consistent with this assumption. In Sec. V we test the self-consistent theory, Eqs. (2) and (27), against an example where the stress is calculated directly using the numerical tools developed in Ref. [7], which verifies that the assumption made describes correctly the Casimir physics of the soft wall.

II. THEORY

Consider a planar material that varies only in the z direction. In this case, the Casimir-force density $\nabla \cdot \sigma$ also points in the z direction, while σ is diagonal, such that σ_{zz} is indeed the only physically relevant stress component. According to Lifshitz theory [7,11],

$$\sigma_{zz} = -\frac{\hbar c}{(2\pi)^2}\int_0^\infty\int_0^\infty (\mathcal{W}-\mathcal{W}_0)\,u\,du\,d\kappa, \tag{3}$$

$$\mathcal{W} = \sum_{\mathrm{p=E,M}} \frac{1}{\nu_\mathrm{p}}\left(u^2+n^2\kappa^2-\partial_z\partial_{z_0}\right)\widetilde{g}_\mathrm{p}\Big|_{z_0\to z}, \tag{4}$$

with κ being the imaginary wave number and u the spatial Fourier component. Going to imaginary wave numbers improves the convergence of the stress [2] as an integral of the spectral stress density $\mathcal{W}$ and, more importantly, describes the broadband nature of the Casimir effect, as each imaginary frequency requires a Hilbert transform of the material parameters over a wide range of real frequencies [2,13]. These parameters are the electric permittivity ε and magnetic permeability μ that give rise to

$$n=\sqrt{\varepsilon\mu}, \quad \nu_\mathrm{E}=\mu, \quad \nu_\mathrm{M}=\varepsilon, \tag{5}$$

for the two polarizations E and M of the electromagnetic field with Fourier-transformed Green functions $\widetilde{g}_\mathrm{p}$ satisfying the inhomogeneous wave equation,

$$\partial_z\frac{1}{\nu_\mathrm{p}}\partial_z\widetilde{g}_\mathrm{p} - \frac{u^2+n^2\kappa^2}{\nu_\mathrm{p}}\widetilde{g}_\mathrm{p} = \delta(z-z_0). \tag{6}$$

The quantity $\mathcal{W}_0$ represents the diverging part in the spectral stress density of the electromagnetic zero-point fluctuations inside the material, which is removed in the renormalization of the Casimir stress, Eq. (3). There we use the point-splitting method [11]: Each point in space is mentally split into two, representing an emitter (at z_0) and a receiver (at z). The emitter sends out an electromagnetic wave; the receiver responds to the part of the electromagnetic wave that is scattered back. In this picture, renormalization amounts to subtracting from the full Green function the part that is purely outgoing such that the scattered part remains. We argued in Ref. [7] that the outgoing wave is given by the geometrical-optics expression of the Green function in the vicinity of the point of emission (up to quadratic order). This procedure was proven [7] to remove the unphysical divergencies of the Casimir stress inside planar media. It also gives a recipe for computing the stress numerically: Fig. 2 shows the stress calculated numerically for a profile with discontinuities in the derivative of the refractive index (details of the calculation are described in Sec. V). One clearly sees the physical divergencies of the stress at the edges that remain after renormalization.

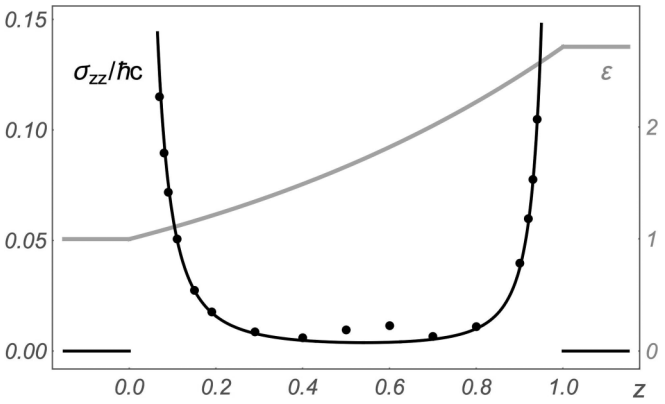

FIG. 2. Casimir stress. Numerical computation (dots) of the Casimir stress σ_{zz} for the profile $\varepsilon(z)$ of the electric permittivity shown (gray curve), $\mu = 1$. The solid black curve shows the sum of our formula for the stress near each edge, Eq. (27), in excellent agreement with the numerical results near the edges. The stress is zero in the constant parts of the profile. We employed the profile of Eq. (28) that includes Lorentzian-type dispersion (in the shown profile of the permittivity we plot ϵ for $\kappa = 0$). Dispersion is necessary for the convergence of the Casimir stress [7].

III. GEOMETRY

For getting an analytic expression of the characteristic behavior of the Casimir stress we apply insights from geometry—transformation optics [14]—combined with the features of Casimir physics. The Casimir stress is given by the reflected waves inside the material and at its boundaries [1–8]. As we are employing waves with imaginary frequencies, their amplitudes are exponentially falling while propagating; waves scattered from distant regions are exponentially suppressed.

We thus only need to consider the immediate vicinity of the point where most of the scattering occurs: the discontinuity of dn/dz. Moreover, there we can replace the actual refractive-index profile [solid line of Fig. 1(a)] by one that also contains the characteristic feature—the discontinuity of dn/dz—but does not cause scattering elsewhere [dotted line of Fig. 1(a)]. As the renormalized stress [7] originates from the scattered part of the Green function, the renormalization becomes trivial: It is equivalent to subtracting from the total Green function the Green function of propagation in the scatteringless refractive-index profile. This argument allows us to calculate the asymptotics of the Casimir stress for all planar refractive-index profiles with $\mu = 1$ having a jump in the derivative of n.

In the following we show that such a scatteringless profile is the one of the Beltrami space [15] [Fig. 1(a), dotted line]:

$$n = -\frac{b}{z} \quad \text{for} \quad z < 0, \tag{7}$$

that describes a maximally symmetric, open space [16] of constant negative curvature for the electromagnetic field if, as in transformation optics [14],

$$\varepsilon = \mu = n. \tag{8}$$

We prove by direct calculation that this profile is scatteringless. Then we show that it remains so in the realistic case of $\varepsilon = n^2, \mu = 1$. To avoid clutter in our calculations we set the spatial units such that

$$b = 1, \tag{9}$$

and reinstate units later.

For the Beltrami profile of Eq. (7) one can solve the equation for the Green function exactly:

$$g = -\frac{e^{-\kappa s}}{2\pi\, c_+ c_-}, \quad s = 2\,\mathrm{artanh}\,\frac{c_-}{c_+}, \tag{10}$$

where

$$c_\pm = \sqrt{x^2 + y^2 + (z \pm z_0)^2}. \tag{11}$$

One verifies that g solves Eq. (6) with $u^2 = -\partial_x^2 - \partial_y^2$ in physical space. One also verifies that s satisfies the eikonal equation $(\nabla s)^2 = n^2$, which proves that s is the geodesic length—the optical path length. From this follows that g is exactly of the form required by geometrical optics, as it depends on frequency only through the exponential factor $\exp(-\kappa s)$ where $\kappa = -i\omega/c$ (with positive imaginary ω in our case): Geometrical optics is exact for the Beltrami profile. Note that this is only true for the profile of Eq. (7) from $-\infty$ to 0 in its entirety. If n turns to a constant at $z = -1$, forming an edge in the profile, the discontinuity in the refractive index will cause scattering, i.e., a violation of geometrical optics, and hence Casimir forces [7].

For the undisturbed profile of Eq. (7) we solve for the Green function in Fourier space, Eq. (6), and obtain for both polarizations:

$$\widetilde{g} = -I_\kappa(-uz_0)K_\kappa(-uz), \tag{12}$$

for $z < z_0$ and z and z_0 interchanged for $z > z_0$, where K and I are the modified Bessel functions [17]. We will make use of this form in the case of realistic profiles with $\varepsilon \neq \mu$ where the interpretation of the material as establishing a geometry for the electromagnetic field is no longer exact [14]. As it turns out in the next section, the Beltrami profile will still be scatteringless.

IV. REALITY

In the remainder of this paper we consider the realistic case of planar media with the Beltrami profile, Eqs. (7), (9), and

$$\varepsilon = n^2, \quad \mu = 1. \tag{13}$$

In this case, the electric and magnetic properties of the material are different, and so the E and M polarizations differ as well:

$$\begin{aligned} \widetilde{g}_\mathrm{E} &= -\sqrt{z_0 z}\, I_\nu(-uz_0)K_\nu(-uz), \\ \widetilde{g}_\mathrm{M} &= -\frac{1}{\sqrt{z_0 z}}\, I_\nu(-uz_0)K_\nu(-uz), \end{aligned} \tag{14}$$

for $z < z_0$ and z and z_0 interchanged for $z > z_0$, while we get for the index,

$$\nu = \sqrt{\kappa^2 + 1/4}. \tag{15}$$

The Green functions for the realistic case of Eq. (13) thus differ from Eq. (12) of the geometric case of Eq. (8) by the prefactors $(z_0 z)^{1/2}$ and $(z_0 z)^{-1/2}$, respectively, which means that they are also scatteringless in space. However, as the index, Eq. (15), is different from κ, their temporal behavior is modulated due to the different dependence on frequency $ic\kappa$; there is geometric dispersion [7]. Yet for the renormalization of the Casimir stress in planar media, geometric dispersion is not relevant [7]; we can thus regard the Green functions (14) as describing the outgoing waves that give rise to $\mathcal{W}_0$ via Eq. (4) and are subtracted in the renormalization of the stress, Eq. (3).

Consider now the full profile of the soft wall [Fig. 1(a)] with $\varepsilon = \mu = 1$ for $z < -1$ and the Beltrami profile of Eq. (7) for $-1 < z < 0$. At the edge of the soft wall, $z = -1$, the derivative jumps from zero to $dn/dz = 1$ in our units ($dn/dz = b^{-1}$ in general). For $-1 < z_0 < 0$ and $z < z_0$ the Fourier-transformed Green functions are given by the outgoing waves of Eq. (14) plus a solution of the homogeneous wave equation:

$$\begin{aligned} \widetilde{g}_\mathrm{E} &= -\sqrt{z_0 z}\, I_\nu(-uz_0)[K_\nu(-uz) + \rho_\mathrm{E} I_\nu(-uz)], \\ \widetilde{g}_\mathrm{M} &= -\frac{1}{\sqrt{z_0 z}}\, I_\nu(-uz_0)[K_\nu(-uz) + \rho_\mathrm{M} I_\nu(-uz)], \end{aligned} \tag{16}$$

with coefficients ρ_E and ρ_M for $-1 < z$, and

$$\widetilde{g}_\mathrm{E} \propto e^{wz}, \quad \widetilde{g}_\mathrm{M} \propto e^{wz}, \quad w = \sqrt{\kappa^2 + u^2}, \tag{17}$$

for $z < -1$. We see from Eq. (6) that at $z = -1$ both $\widetilde{g}$ and $\partial_z \widetilde{g}$ must be continuous (the latter, because ε and μ are continuous there). As the outgoing waves are the $I_\nu(-uz_0)K_\nu(-uz)$ waves we simply drop them in the renormalization and use only the reflected waves in Eqs. (3) and (4) of the Casimir stress. In this way we obtain

$$\sigma_{zz} = -\frac{\hbar c}{(2\pi)^2} \int_0^\infty \int_0^\infty (\rho_\mathrm{E}\mathcal{W}_\mathrm{E} + \rho_\mathrm{M}\mathcal{W}_\mathrm{M}) u\, du\, d\kappa, \tag{18}$$

with $\mathcal{W}_{\rm E}$ and $\mathcal{W}_{\rm M}$ given by

$$\begin{aligned}\mathcal{W}_{\rm E} &= -(n^2\kappa^2 + u^2 - \partial_z\partial_{z_0})\sqrt{z_0 z}\, H\Big|_{z_0\to z},\\ \mathcal{W}_{\rm M} &= -\frac{1}{\varepsilon}(n^2\kappa^2 + u^2 - \partial_z\partial_{z_0})\frac{1}{\sqrt{z_0 z}}\, H\Big|_{z_0\to z},\end{aligned} \tag{19}$$

and $H = I_\nu(-uz_0)I_\nu(-uz)$. For evaluating the integrals in Eq. (18) we use polar coordinates,

$$\kappa = w\cos\theta, \quad u = w\sin\theta, \tag{20}$$

and the asymptotics of the integrand in the limit of $w\to\infty$, as a rapid growth of the stress in physical space corresponds to large components in Fourier space. We thus replace the modified Bessel functions by their uniform asymptotics for both order ($\nu\sim\kappa$) and argument ($x\propto u$) [17]:

$$\begin{aligned}K_\nu(x) &\sim \sqrt{\frac{\pi}{2}}\frac{e^{-\sqrt{\nu^2+x^2}+\nu\,\mathrm{arsinh}(\nu/x)}}{\sqrt[4]{\nu^2+x^2}},\\ I_\nu(x) &\sim \frac{e^{\sqrt{\nu^2+x^2}-\nu\,\mathrm{arsinh}(\nu/x)}}{\sqrt{2\pi}\sqrt[4]{\nu^2+x^2}},\end{aligned} \tag{21}$$

and obtain for the $\mathcal{W}_{\rm E}$ and $\mathcal{W}_{\rm M}$ of Eq. (19) in the limit of $w\to\infty$ the expressions:

$$\begin{aligned}\mathcal{W}_{\rm E} &\sim -\frac{\cos^2\theta}{2\pi z\,[z^2-(z^2-1)\cos^2\theta]}\,e^{2w\phi(z)},\\ \mathcal{W}_{\rm M} &\sim \frac{2z^2+(1-2z^2)\cos^2\theta}{2\pi z\,[z^2-(z^2-1)\cos^2\theta]}\,e^{2w\phi(z)},\end{aligned} \tag{22}$$

with the exponent given by

$$\phi(z) = \sqrt{\cos^2\theta + z^2\sin^2\theta} + \cos\theta\,\mathrm{arsinh}\frac{\cot\theta}{z}. \tag{23}$$

We also solve for $\rho_{\rm E}$ and $\rho_{\rm M}$ as follows: Since $\partial_z\widetilde{g} = w\widetilde{g}$ for $\widetilde{g}$ of Eq. (17) for $z<-1$, continuity of $\widetilde{g}$ and $\partial_z\widetilde{g}$ requires that the same is true for $\widetilde{g}$ of Eq. (16) at $z=-1$, which establishes a linear equation for each $\rho_{\rm p}$. Using the asymptotics of the modified Bessel functions, Eq. (21), gives in the limit of $w\to\infty$:

$$\begin{aligned}\rho_{\rm E} &\sim -\frac{\pi\cos^2\theta}{4w}\,e^{-2w\phi(-1)},\\ \rho_{\rm M} &\sim \frac{\pi(2-\cos^2\theta)}{4w}\,e^{-2w\phi(-1)}.\end{aligned} \tag{24}$$

Next we consider the asymptotics for $z\to-1$ in the integral of Eq. (18) for the stress. The convergence of the integral is controlled by the exponents in Eqs. (22) and (24), hence we take $\phi(z)-\phi(-1)\sim-(z+1)$ to first order in $z+1$ from Eq. (23), while for the prefactors we put $z=-1$. We substitute $\zeta=\cos\theta$ and obtain

$$\begin{aligned}\sigma_{zz} &= \frac{\hbar c}{16\pi^2}\int_0^\infty e^{-2w(z+1)}w\,dw\int_0^1(2-2\zeta^2+\zeta^4)d\zeta\\ &= \frac{23}{960\pi^2}\,\frac{\hbar c}{(z+1)^2}.\end{aligned} \tag{25}$$

Writing $a=z+1$ and reinstating units gives the main result of this paper, Eq. (2). It is elementary to generalize it to the case when a material with uniform refractive index n_0 different from unity meets a soft wall. We simply put the edge of the Beltrami profile $n=-1/z$ at $z=-1/n_0$, and express $n_0\kappa$ instead of κ as $w\cos\theta$. We obtain along the same lines as above:

$$\sigma_{zz} = \frac{23n_0}{960\pi^2}\,\frac{\hbar c}{\left(z+n_0^{-1}\right)^2}. \tag{26}$$

As the first derivative of the Beltrami profile $-1/z$ is n_0^2 at $z=-1/z_0$, this corresponds to $b=1/n_0^2$. Hence we obtain in general units,

$$\sigma_{zz} = \frac{23}{240\,(2\pi)^2 n_0^3}\,\frac{\hbar c}{a^2b^2}. \tag{27}$$

Finally, in the case the first derivative of n does not rise, but drops by $-b^{-1}$ at the edge we follow a similar procedure, and obtain the same result.

Note that our result is only valid when dispersion, the frequency dependence of ε and μ, is not important in the relevant range of w. Ultimately, dispersion will soften the singularity of the Casimir stress near the edge, but it will not completely remove it, as the integral over the spatial Fourier components in Eq. (3) remains divergent there. Our numerical results (Fig. 2) show that our analytic formula, Eq. (2), describes well the intermediate regime near the edge until dispersion softens the power law.

V. EXAMPLE

To check our theory we compare it to a calculation of the Casimir stress according to the renormalization prescription of Ref. [7] in a material with a jump in the derivative of the permittivity:

$$\varepsilon = \begin{cases}1 & z<0\\ \epsilon^z & 0\leqslant z\leqslant 1,\\ \epsilon & 0<z\end{cases} \qquad \epsilon = \frac{\kappa^2+e\kappa_0^2}{\kappa^2+\kappa_0^2}, \tag{28}$$

($\kappa_0=200$, solid gray curve in Fig. 2 plotted for $\kappa=0$) and $\mu=1$. Equation (28) describes a dispersive inhomogeneous permittivity profile with a Lorentzian dispersion relation for imaginary frequencies with a resonance at κ_0. The Green functions in an exponential profile are derived in Ref. [6]. We evaluate numerically the spectral stress density as defined in Eq. (4); subtracting $\mathcal{W}_0$ we then integrate to find σ_{zz} according to Eq. (3). The stress in the homogeneous external shoulders of the profile ($z<0$ and $1<z$) is zero [18], the stress in the inhomogeneous region is plotted (Fig. 2, black dots). The asymptotic stress given by Eq. (27) for the two soft boundaries at $z=0$ and $z=1$ are summed and also plotted (black curved) in Fig. 2. One sees that close to the boundaries the asymptotic formula captures beautifully the behavior of the stress. However, for smaller a, closer to the jump in the permittivity's derivative, the spectral density contributes to the stress at greater frequencies. For $\kappa\sim40$ the jump in the derivative of the permittivity already varies by 5% with respect to its value at $\kappa=0$, for which the asymptotic stress is calculated. We thus find numerically that the asymptotic formula is correct to within 10% for $a\in[0.05,0.15]$ in our arbitrary units.

VI. SUMMARY

Only recently, one can calculate the Casimir stress inside materials [7]. We have found that the stress grows with a characteristic power law, Eq. (2), near the edge of a soft wall [8] where the first derivative of the refractive index is discontinuous. The final formula, Eq. (27), represents one of the few analytic results in the theory of Casimir forces [19]. Of course, the jump in the first derivative of n is an idealization, and so is the resulting divergence. However, our final result, Eq. (27), will still describe the leading asymptotics of the Casimir stress until material dispersion softens it, as our numerical example has shown. Ultimately, the molecular structure of the material will make the stress finite due to spatial dispersion. Nevertheless, the stress will remain large, because the molecular structure can only affect spatial Fourier components in the spectral stress density that are comparable to the molecular size. Our result also gives a first glimpse on new phenomena related to the aggregation of materials by Casimir (van der Waals) forces at surfaces. Our paper answers the question of how such forces behave near edges of the refractive-index profile, but it also raises many more questions that may inspire future research. For example, what is the best way of measuring such forces? What are stable configurations of aggregated materials? What are the time scales of aggregation? How does diffusion compete with Casimir (van der Waals) forces?

ACKNOWLEDGMENTS

We thank Y. Drori, M. Fink, and E. Shahmoon for stimulating discussions. I.G. is grateful to the Azrieli Foundation for the award of an Azrieli Fellowship. Our work was also supported by the European Research Council and the Israel Science Foundation, a research grant from Louis Rosenmayer and from J. Nathan, and the M. B. Koffler Professorial Chair.

[1] H. B. G. Casimir, Kon. Ned. Akad. Wetensch. Proc. **51**, 793 (1948).

[2] A. W. Rodriguez, F. Capasso, and S. G. Johnson, Nat. Photon. **5**, 211 (2011).

[3] M. T. H. Reid, A. W. Rodriguez, J. White, and S. G. Johnson, Phys. Rev. Lett. **103**, 040401 (2009).

[4] W. M. R. Simpson, *Surprises in Theoretical Casimir Physics* (Springer, Berlin, 2014).

[5] I. E. Dzyaloshinskii and L. P. Pitaevskii, Sov. Phys. JETP **9**, 1282 (1959); M. Bordag and D. V. Vassilevic, J. Phys. A **32**, 8247 (1999); M. Bordag, K. Kirsten, and D. Vassilevich, Phys. Rev. D **59**, 085011 (1999); S. Goto, R. W. Tucker, and T. J. Walton, Proc. SPIE **8072**, 80720O (2011); W. M. R. Simpson, S. A. R. Horsley, and U. Leonhardt, Phys. Rev. A **87**, 043806 (2013); F. Bao, B. Luo, and S. He, *ibid.* **91**, 063810 (2015); F. Bao, J. S. Evans, M. Fang, and S. He, *ibid.* **93**, 013824 (2016); R. J. Churchill and T. G. Philbin, Phys. Rev. B **94**, 235422 (2016); see also Refs. [6] and [8], and the attempts to renormalize the vacuum energy-momentum tensor of the electromagnetic field in general relativity, S. L. Adler, J. Lieberman, and Y. J. Ng, Ann. Phys. (NY) **106**, 279 (1977); R. M. Wald, Phys. Rev. D **17**, 1477 (1978), which, via the connection between geometries and media [14], is related to the renormalization of the Casimir force in materials.

[6] T. G. Philbin, C. Xiong, and U. Leonhardt, Ann. Phys. (NY) **325**, 579 (2010).

[7] I. Griniasty and U. Leonhardt, Phys. Rev. A **96**, 032123 (2017).

[8] M. Bordag and D. V. Vassilevich, Phys. Rev. D **70**, 045003 (2004); K. A. Milton, *ibid.* **84**, 065028 (2011); J. D. Bouas, S. A. Fulling, F. D. Mera, C. S. Trendafilova, K. Thapa, and J. Wagner, in *Spectral Geometry*, edited by A. H. Barnett, C. S. Gordon, P. A. Perry, and A. Uribe, Proceedings of Symposia in Pure Mathematics **84**, 139 (2012); F. D. Mera, S. A. Fulling, J. D. Bouas, and K. Thapa, J. Phys. A **46**, 195302 (2013); K. A. Milton, S. A. Fulling, P. Parashar, P. Kalauni, and T. Murphy, Phys. Rev. D **93**, 085017 (2016); S. W. Murray, C. M. Whisler, S. A. Fulling, J. Wagner, H. B. Carter, D. Lujan, F. D. Mera, and T. E. Settlemyre, *ibid.* **93**, 105010 (2016).

[9] The other nonvanishing components of the stress, σ_{xx} and σ_{yy}, do diverge there, but they do not contribute to the force density $\nabla \cdot \sigma$, as they depend only on z.

[10] A classic experiment exhibiting both Casimir attraction and repulsion is that of two dielectric solids, with n_1 and n_3, immersed in a liquid with refractive index n_2; see J. N. Munday, F. Capasso, and V. A. Parsegian, Nature (London) **457**, 170 (2009); If $n_1 < n_2 < n_3$ or $n_1 > n_2 > n_3$, the Casimir force between the bodies is repulsive. If n_1,$n_3 > n_2$ or n_1,$n_3 < n_2$ the Casimir force is attractive (which is the commonly observed effect in vacuum, $n_2 = 1$). The leading asymptotics, Eq. (2), of the internal Casimir force density inside a soft wall between either of the bodies is indifferent to the interaction with the second body, as well as to whether $n_1 > n_2$ or $n_1 < n_2$.

[11] E. M. Lifshitz, Zh. Exp. Theor. Fiz. **29**, 94 (1956); see also Ref. [12] and L. D. Landau and E. M. Lifshitz, *Statistical Physics, Part 2* (Pergamon, Oxford, 1980).

[12] I. E. Dzyaloshinskii, E. M. Lifshitz, and L. P. Pitaevskii, Adv. Phys. **10**, 165 (1961).

[13] J. N. Munday and F. Capasso, Phys. Rev. A **75**, 060102(R) (2007).

[14] U. Leonhardt and T. G. Philbin, *Geometry and Light: The Science of Invisibility* (Dover, Mineola, 2010).

[15] T. Needham, *Visual Complex Analysis* (Clarendon Press, Oxford, 2002).

[16] A. Zee, *Einstein Gravity in a Nutshell* (Princeton University Press, Princeton, 2013).

[17] A. Erdélyi, W. Magnus, F. Oberhettinger, and F. G. Tricomi, *Higher Transcendental Functions* (McGraw-Hill, New York, 1981).

[18] In planar media, the Casimir stress due to a single reflection is zero [7]. In the homogeneous region of the profile [Fig. 1(a)] only one reflection occurs—from the edge of the inhomogeneous profile, and so σ_{zz} vanishes for $z < 0$. Note that in the inhomogeneous region geometric dispersion [7] plays the role of the second reflection, which creates a nonvanishing stress.

[19] Reference [1] and T. H. Boyer, Phys. Rev. A **9**, 2078 (1974); K. A. Milton, Ann. Phys. (NY) **127**, 49 (1980); U. Leonhardt and W. M. R. Simpson, Phys. Rev. D **84**, 081701(R) (2011).